Polyethersulfone–[Silicon Oxide] Hybrid Materials via *In Situ* Sol–Gel Reactions for Tetra-Alkoxysilanes

N. JUANGVANICH, K. A. MAURITZ

Department of Polymer Science, University of Southern Mississippi, Hattiesburg, Mississippi 39406-0076

Received 17 March 1997; accepted 4 September, 1997

ABSTRACT: Polyethersulfone (PES)–[silicon oxide] hybrids were derived via sol–gel reactions for tetraethoxysilane (TEOS) and tetramethoxysilane (TMOS) in dimethylacetamide solutions of the polymer. In one scheme, water was initially present, and condensation reactions between SiOR groups competed with their reactions with —OH groups at PES chain ends. In a second scheme, water addition was delayed; TMOS molecules reacted with chain ends before competing TMOS–TMOS reactions occurred. A third study involved parallel experiments, as follows: 1) introduction of EtOH to PES–TEOS solutions for a time before water addition; and 2) reactions occurring for a time in non-EtOH-containing PES–TEOS solutions before water addition. Infrared (IR) spectroscopy uncovered signatures of Si–O–Si bridges in silicon oxide phases and PES endgroup modifications (Si–O–Ph). Composites prepared according to the latter two schemes contain more Si–O–Ph linkages than those generated via the first. Differential scanning calorimetry showed that T_g can be raised, and thermogravimetric analysis revealed how the PES thermal degradation profile can be modified via these inorganic incorporations. The schemes for late water addition produced composites having increased elongation-to-break and lowered strength relative to unfilled PES. © 1998 John Wiley & Sons, Inc. J Appl Polym Sci **67:** 1799–1810, 1998

Key words: polyethersulfone; silicon oxide; sol-gel reactions

INTRODUCTION

In earlier work, Mauritz and Ju formulated poly(arylene ether sulfone)–[silicon oxide] hybrid materials via sol–gel reactions for tetraethoxysilane (TEOS) in dimethylformamide solutions in which the polymer was also dissolved.[1] The polymer utilized was poly[ether-ether-sulfone-*co*-ether-sulfone] (PEES–PES). In addition to acid-catalyzed hydrolysis–condensation reactions among TEOS molecules, the following condensation reactions of SiOR (R = H, $-CH_2CH_3$) groups with the —OH groups at the PEES–PES chain ends occurred:

$$\equiv Si-OR + HO-(PEES-PES)-OH \rightarrow \equiv Si-O-(PEES-PES)-OH + ROH$$

The crosslinking of PEES–PES chains through the end groups via SiO_4, bridging units, depicted in Figure 1, was strongly indicated, especially by gel permeation chromatography (GPC) analysis. The polymer T_g increased, and thermal degradative stability was enhanced with increasing silicon oxide content. Tensile modulus and strength also increased with increasing inorganic content. However, these amorphous high T_g polymers, being of rather low molecular weight (M_n = 5100), were brittle and lacked the toughness required for high-performance applications. In these previous studies (as well as those reported here), these systems are considered within the limited context of models for studying interactions between poly-

Correspondence to: K. A. Mauritz.

Contract grant sponsors: Mississippi NSF EPSCOR; Petroleum Research Fund (Type AC)

Journal of Applied Polymer Science, Vol. 67, 1799–1810 (1998)

 CCC 0021-8995/98/101799-12

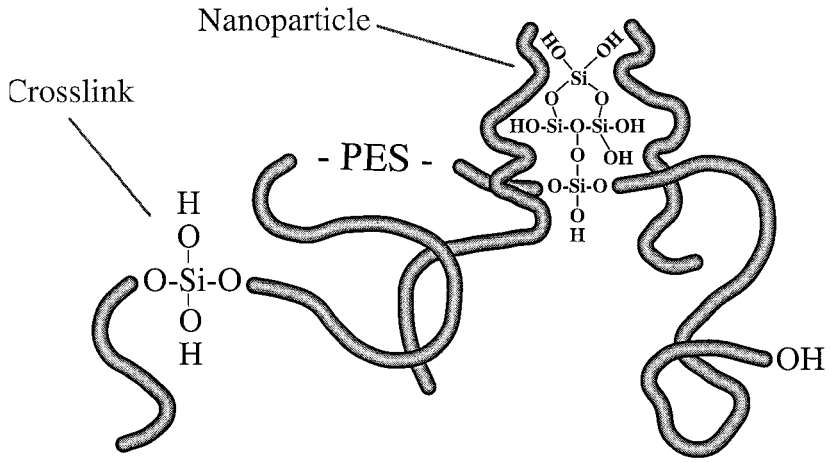

Figure 1 Rough depiction of poly(ether sulfone) chains that are crosslinked through the endgroups via Ph–O–Si–O–Ph bridges. A particle has grown via condensation reactions of an alkoxysilane from such a bridge on the right side of the figure.

(arylene ether sulfone) polymers and incorporated silicon oxide phases. The work outlined in this article is a continuation of this earlier effort and utilizes PES (rather than a PEES–PES copolymer), of a higher molecular weight, where —OH endgroups are again present, as follows:

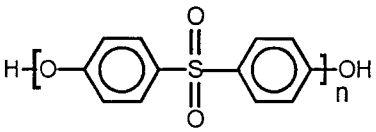

Sol-gel reaction schemes for TEOS and tetramethoxysilane (TMOS), with water added at different times, are described in this article. The results presented here derive from studies that were rather exploratory in nature, and more detailed investigations are needed to identify materials that are optimal with regard to properties. Of particular interest with regard to this class of high-performance polymers is the elevation of T_g. If restrictions are placed on long-range chain segmental mobility by this inorganic modification, it might be reasoned that the temperature of the onset of thermal degradation is correspondingly increased. To be sure, other factors (for example, critical chemical bond strengths, presence of O_2) are also involved in degradation.

RESULTS

Scheme I: Immediate Water Addition Procedure

Composite Formulation

Materials. OH-terminated PES (M_n = 12,800, M_w = 26,600) resin was provided by ICI PLC. The polymer, in powder form, was used as received. TEOS and the solvent *N*,*N*-dimethylacetamide (DMAc) (Aldrich Co.) were used as received. Concentrated HCl (Fisher Co.) was diluted to 0.121*N* in DMAc for each experiment.

Organic / Inorganic Composite Formulation. A series of composites was formulated for different TEOS : PES mole ratios. All solution compositions, listed in Table I, have mole ratios TEOS : H_2O = 1 : 4 and TEOS : HCl = 1 : 0.0022.

PES was completely dissolved in DMAc to give a 20 wt % solution, and the sol-gel reagents were subsequently added. First, TEOS was added, followed by distilled water. Finally, HCl addition catalyzed both the hydrolysis of TEOS and condensation of TEOS with OH-terminated polymer chains. The solution was stirred during mixing and then refluxed and stirred for 6 h at 40°C. After 6 h, the solutions were poured into petri dishes and were well covered with aluminum foil, in which a few needle holes were placed to keep an

Table I Reactive Solution Compositions for Hybrid Formulation

TEOS : PES (mol : mol)[a]	PES (g)	TEOS (μL)	H_2O (μL)	HCl (mL)	DMAc (mL)
90 : 10	2.0	310	100	0.26	10.0
74 : 26	2.0	100	32	0.26	10.0
50 : 50	2.0	35	11	0.26	10.0
35 : 65	2.0	19	6	0.26	10.0

[a] Molar ratio per PES chain.

excess vapor pressure above the reacting solutions so as to prevent sample cracking. DMAc was evaporated from the samples at 60°C in an oven, and the films gradually solidified. A pure PES film, meant to be a control sample, was cast as in the procedure described above, but without addition of the sol-gel reagents.

Prior to characterization, every sample was dried at 160°C (DMAc boiling point) for 2 days to remove residual solvent. In handling, the composite films were observed to be very brittle and appeared white by simple optical inspection as well as in a light microscope. This suggests phase separation on a dimensional level greater than the wavelength of light.

Characterization

Fourier Transform Infrared Spectroscopy. IR reflectance spectra were obtained using a Bruker IFS 88 Fourier transform infrared FTIR spectrometer using 4 cm^{-1} resolution and a thallium bromide–thallium iodide KRS-5 ATR plate. It was necessary to utilize reflectance rather than transmission spectra, owing to the high absorbance of these samples having these particular thicknesses (somewhat less than 1 mm). A total of 200 interferograms was taken for each sample. Difference spectra, that is, PES–(silicon oxide) – unfilled PES, were derived for the purpose of enhancing bands reflective of the inorganic component by subtracting the bands for pure PES. When performing ATR spectral subtraction in this way, total elimination of the pure polymer bands is not always possible, owing to somewhat different penetration depths and indices of refraction of an IR beam at these wavenumbers. Despite the remnants of polymer bands after some subtractions, the signature bands of the inorganic inclusions are enhanced in this way, and, at the least, qualitative analysis is possible, as seen in earlier similar studies.[2–7] Finally, attenuated total reflectance (ATR) is a probe of near-surface regions, and caution should be exercised in extrapolating spectroscopic interpretations to conclusions regarding bulk structure. This question will be explored in future studies involving very thin samples for which it is possible to obtain transmission spectra.

^{29}Si Nuclear Magnetic Resonance Spectroscopy. Limited ^{29}Si solid-state nuclear magnetic resonance (NMR) studies were performed on the composites produced according to Scheme III, as described below. Of particular interest is the chemical shift distribution in the Q region, in which peaks can reside that are diagnostic of the degree of Si atom substitution around SiO_4 tetrahedra, i.e., $Q^n = (RO)_{4-n}Si(OSi)_n$.

A Bruker MSL-400 spectrometer that used a standard 4 mm double-air bearing probe was employed in these experiments. Ground samples were packed into zirconia rotors sealed with Kel-F™ caps and spun at a rate of 3.3–3.8 kHz. The standard cross-polarization–magic angle spinning (CP–MAS) technique[8] was used with high-power proton decoupling implemented during data acquisition. The acquisition parameters were as follows: The ^{1}H 90° pulse width was 5.5 μs, cross-polarization contact time was 3 ms, the dead time delay was 13 μs, and the acquisition time was 45 ms. A recycle delay of 5 s between scans was utilized with $\sim$ 7000–17,000 scans acquired for each sample. All chemical shifts were referenced to the downfield peak of tetrakis(trimethylsilyl)silane (−9.8 ppm with respect to tetramethylsilane (TMS)).

Differential Scanning Calorimetry. Differential scanning calorimetry (DSC) scans were obtained with a DuPont 910 DSC instrument with a heating rate of 20°C/min over the range 25–400°C, under N_2 atmosphere. Samples weighing $\sim$ 10–20 mg were used for each measurement. Samples were heated to 400°C and immediately cooled with liquid N_2. Second scans were obtained as soon as the temperature reached 25°C. Owing to volatiles that evolve during the first scan, through either solvent release or additional, thermally driven condensation reactions between SiOH groups, only second scans are reported.

Thermogravimetric Analysis. Thermogravimetric analysis (TGA) measurements were carried out using a DuPont 951 TGA instrument with a heating rate of 10°C/min over the range of 50–800°C under N_2 atmosphere. Samples, typically weighing 10–20 mg were placed in a platinum pan and weighed on the TGA balance to within ± 1 μg.

Mechanical Tensile Analysis. Stress versus strain tests were performed for selected samples at 25°C using an MTS 810 Universal Test Machine operating at a speed of 0.3 mm/s, using a 100 lb load cell. Test samples were 35 mm long by 5 mm wide, with a spacing between the clamps of 20 mm.

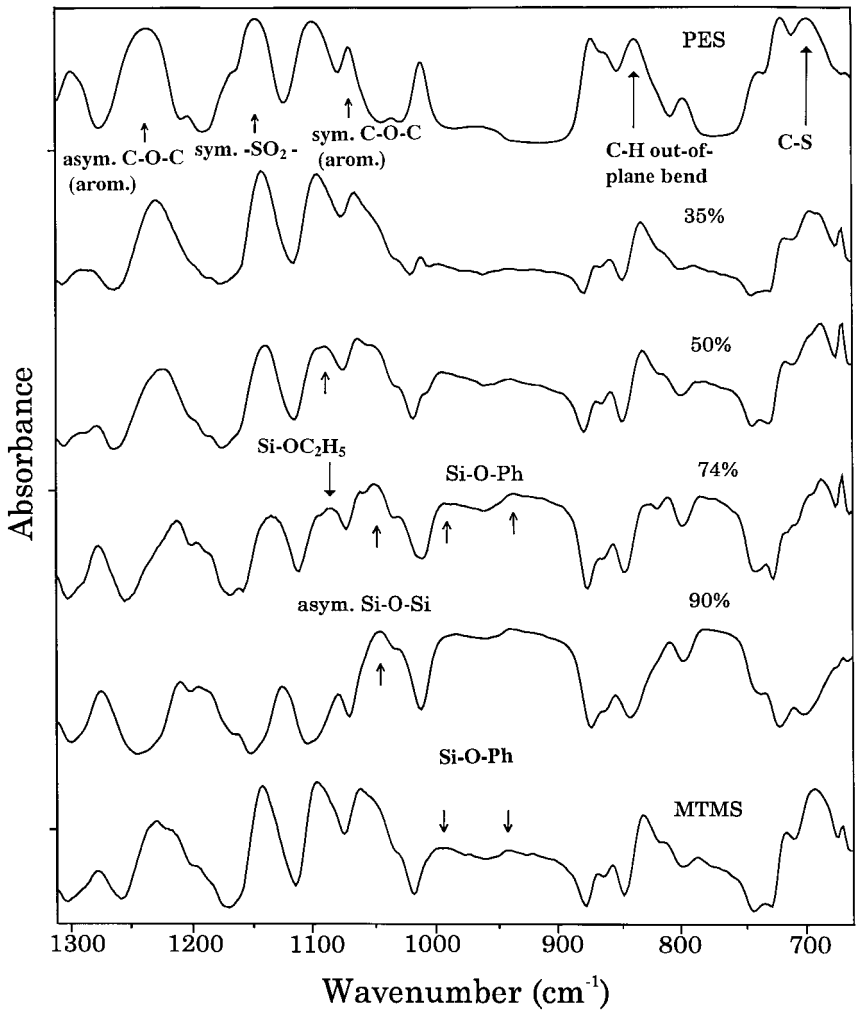

Figure 2 FTIR–ATR subtraction spectra for PES–[silicon oxide] hybrids with indicated initial TEOS mole percent compositions, formulated according to Scheme I. Fingerprint bands of the silicon oxide component and selected PES bands are labeled. Also shown are the spectrum of pure PES and of PES subjected to acid-catalyzed reactions with methoxytrimethylsilane (MTMS) without water (bottom).

RESULTS

FTIR Spectroscopy. The spectra for the hybrids, with indicated initial TEOS mole percent compositions, [TEOS/(TEOS + PES)] × 100%, are displayed in Figure 2. We will confine our discussion to those bands that are fingerprints of the silicon oxide component and polymer bands that appear to be affected by this component.

The subtraction spectra for the 50, 74, and 90% composites showed two bands, at ~ 990 and ~ 940 cm^{-1}, that are not present in the spectrum of pure PES (top). Therefore, these bands are attributed to the silicon oxide phase. The absence of this faint feature for the 35% hybrid is most likely due to low detection sensitivity. These two bands are assigned to Si–O–Ph linkages, based on prior spectroscopic studies of simpler model compounds.[9–14] Given this assignment, the important fact that TEOS has reacted with the PES endgroups is established. This fact, in turn, suggests that covalent linkages exist between the organic and inorganic phases, although more evidence is required to substantiate this broader assertion. Reinforcing this conclusion is the presence of the two Si–O–Ph bands in the spectrum (bottom) for a material produced in similar fashion via acid-catalyzed alcoholysis reactions between PES and methoxytrimethylsilane (MTMS), but without water addition. This reaction involves

only —OH groups at the ends of PES chains and the single alkoxide group of $(H_3C)_3SiOCH_3$ molecules. Complications involving PES crosslinking through endgroups as well as the construction of an interlinked silicon oxide phase are not introduced by the reaction of this monofunctional species. In particular, the Si–O–Ph bands cannot be confused with the Si–OH stretching band that would be present in this region if water were present. Other observed peaks appear to be due to PES bands[14,15] that have been incompletely subtracted, although these peaks become progressively weaker with an increasing percentage of TEOS as is reasonable. A number of PES bands are indicated in Figure 2.

The Si–O–Ph band absorbances increase as the percentage of TEOS increases, indicating that more endgroups are reacted. For 35 and 50% TEOS, these absorbances are relatively low, and peaks for pure PES are seen in the spectrum.

In the 35% spectrum, there is a shoulder on the right side of the band for symmetric aromatic C–O–C vibration. This feature, situated at $\sim$ 1050 cm^{-1}, is absent from the pure PES spectrum and becomes increasingly stronger with an increasing percentage of TEOS. Moreover, a shoulder develops on the right side of this band. These two components are attributed to asymmetric stretching in Si–O–Si groups. In earlier reports of the IR spectroscopic characterization of Nafion®–[silicon oxide] nanocomposite membranes, it was pointed out that these components correspond to Si–O–Si groups in cyclic (high wavenumber) and linear (low wavenumber) configurational subunits.[2–6] Given this interpretation, it appears that the silicon oxide phase becomes more linear, as opposed to crosslinked, with an increasing TEOS percentage. A band at around 1090 cm^{-1} becomes increasingly prominent in proceeding from the 50 to the 90% composite. This is exactly in the position of $Si–OC_2H_3$ stretching. While this band reflects unhydrolyzed alkoxide groups and appears more distinct with an increasing percentage of TEOS, its absorbance diminishes relative to that of the Si–O–Si peak. It is interesting that the Si–OH stretching band, which can occur with considerable variation around 950 cm^{-1}, is either absent or too weak to be detected for these samples. We do not believe that the low wavenumber band ($\sim$ 940 cm^{-1}) attributed to Si–O–Ph groups is confused with the Si–OH band. The reason for this view is that the spectrum, in the region 1000–900 cm^{-1}, of PES reacted exclusively with MTMS with no added water, is very similar to spectra corresponding to the composites formulated using TEOS and water. Therefore, we conclude that while SiOEt groups are present (as indicated by the 1090 cm^{-1} band), SiOH groups do not exist in significant abundance.

The strong peak at 1150 cm^{-1} for pure PES (top spectrum) is due to symmetric vibration of the $—SO_2—$ group.[14] This incompletely subtracted band shifts down to $\sim$ 1125 cm^{-1} with an increasing percentage of TEOS. It is unlikely that this shift is artificially due to the subtraction procedure because it occurs monotonically rather than in random fashion, and there are no interfering silicon oxide bands in the vicinity. It is reasonable to attribute this shift to an increasing number of interactions between the silicon oxide component and $—SO_2—$ groups. This would imply that a significant fraction of the silicon oxide phase is distributed along the chain in addition to residing at the chain ends, although the absence of the Si–OH band is at odds with this notion. The band at $\sim$ 1230 cm^{-1} seen in the spectrum for pure PES is in the position where the C–O stretch in phenols is located, and these groups are certainly present, albeit only at the chain ends.[14] The aromatic C–O–C asymmetric vibration also lies in this region.[14] Owing to their overwhelming number, we conclude that the 1230 cm^{-1} band is dominated by these rather than phenolic endgroups. This band also shifts to lower wavenumbers with an increasing percentage of TEOS; and the same general comments regarding interactions of this group with the silicon oxide phase, as were made for $—SO_2—$ groups, can be offered for consideration.

Differential Scanning Calorimetry. DSC curves for pure PES and the composites are shown in Figure 3. The curve for pure PES shows T_g to be $\sim$ 210°C, which is near the value reported by Attwood et al. for this polymer, although the exact value depends on molecular weight.[16] T_g values for all the composites (defined in terms of temperature-at-inflection) are higher than 210°C. However, the composites having the lowest silicon oxide contents (35, 50%) have T_g values higher than those with the highest contents (74, 90%). We speculate that at low uptakes, the chain segmental mobility of PES chains is restricted through endgroup linking by SiO_4 bridges. The same might be said for the remaining hybrids, except that at higher silicon oxide levels, larger invasive silicon oxide particles act as packing defects that create considerable free volume, thereby lowering

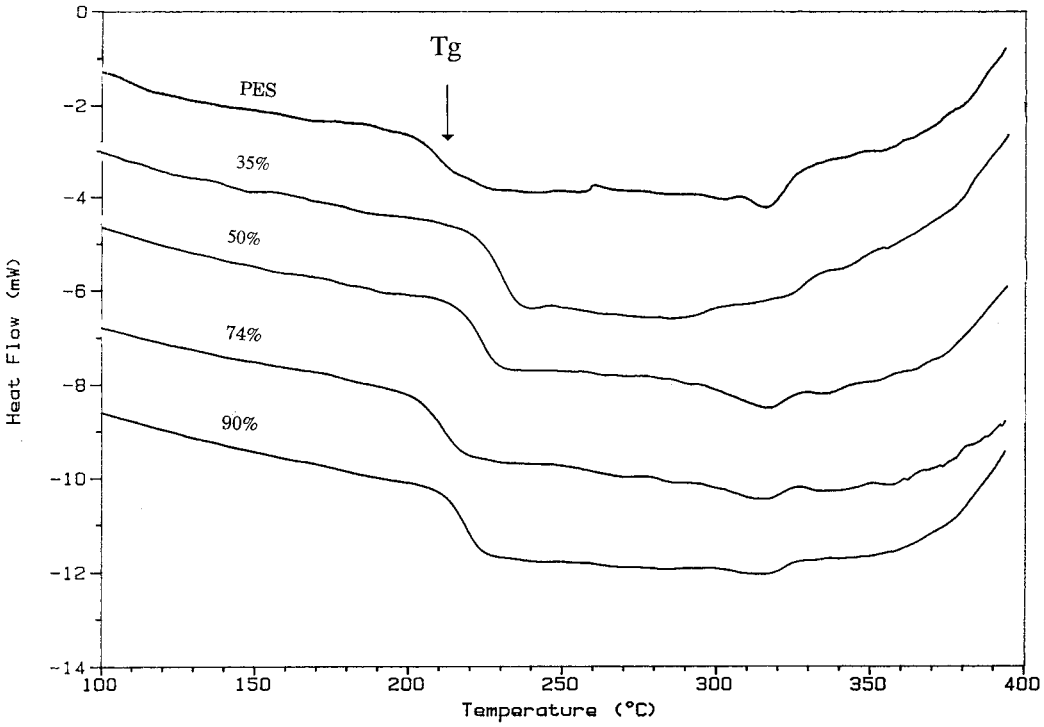

Figure 3 DSC curves (20°C/min) for pure PES and composites having indicated initial TEOS compositions.

T_g. For the 50% composite, there will be only one TEOS molecule, on the average, available to connect two chain ends (theoretical 100% crosslinking). However, it is more probable that some endgroups will remain unreacted, whereas, in other locations, TEOS molecules might undergo condensation reactions with previously established Ph–O–Si(OR)$_2$–O–Ph linkages. Also, TEOS molecules may react with themselves to the exclusion of reactions with endgroups. For the 90% hybrid, there are, on the average, nine TEOS molecules available to react with the endgroups; this excess would result in nanoparticle formation.

Thermogravimetric Analysis. The thermal degradation of PES, as well as the composites, occurs in three steps, as seen in Figure 4. Each degradation temperature listed in Table II refers to the peak on the corresponding derivative mass loss curve. On comparing Figure 4 with Figure 3, the first mass loss event for pure PES occurs just after the glass transition has been completed. For the composites, all first-step degradation temperatures are lower than that for pure PES. Perhaps this step involves solvent release, as all samples were solvent-cast films, which would be more severe for the hybrids, owing to additional volatiles evolving by the mechanism of thermally driven condensation reactions between SiOEt–SiOH groups. The fact that this loss is most severe for the 90% sample, as well as the fact that it occurs at the lowest temperature for all the composites, would tend to support this hypothesis. On the other hand, all second-step temperatures are higher than that for pure PES, the greatest being that for the 90% hybrid, an order which is the reverse of that for the first step. Interestingly, the third degradative step, with regard to the onset, inflection point, and ending temperatures, is not greatly affected by the presence of the silicon oxide phase. This temperature for pure PES (551°C) is not far from that reported by Crossland et al.,[17] as derived from their TGA studies of PES (537°C), also conducted under N_2. Differences between their values and ours are likely due to differences in molecular weight, as well as the fact that their samples did not involve casting a film from a solvent. The primary mode of degradation is thermal rather than oxidative. Pyrolysis gas chromatography–mass spectroscopy (GC–MS) studies indicate that the most abundant degradation product is diphenylsulfone, with lesser amounts of diphenylether, diphenyl, and phenol, for constant

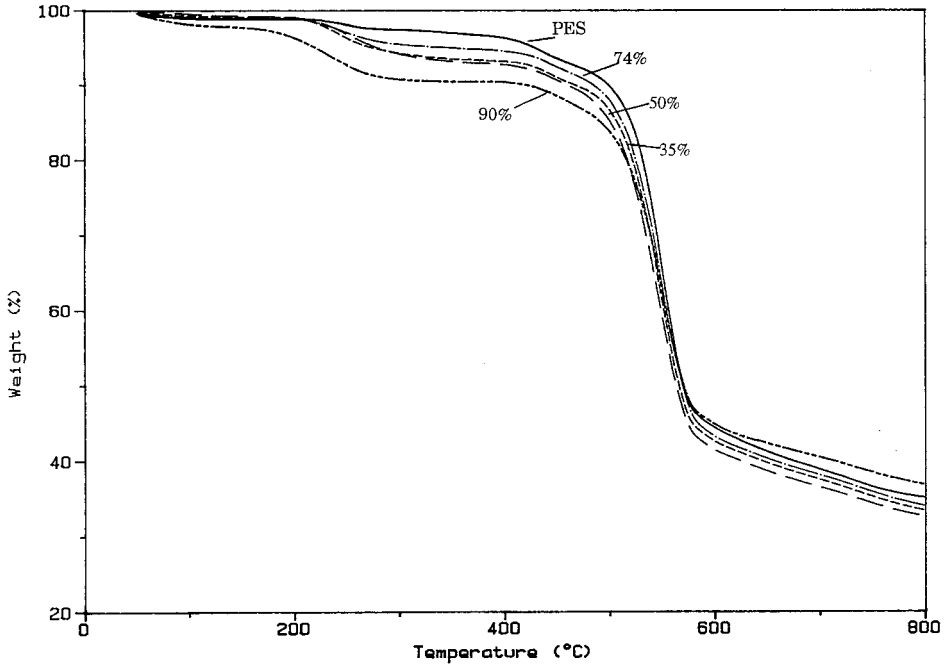

Figure 4 Thermogravimetric scans (10°C/min) for pure PES and composites having indicated initial TEOS compositions.

temperatures up to 550°C. However, diphenylsulfone did not appear at this temperature when the sample was previously heated at 250°C, and SO_2 was detected at 400°C; degradation is affected by prior heating.[17]

The last, most profound step for the composites corresponds to degradation of the organic phase. If this is considered alongside the fact that the temperature of degradation is not greatly altered by the presence of the inorganic phase, it appears that organic–inorganic phase interactions do not greatly influence degradation, although a detailed real-time analysis of the gas products would be necessary to illuminate this issue. Moreover, this statement must be reconciled with the IR spectroscopic evidence, which suggests that there are interactions, not only at the chain ends, but also along the PES chains, with the silicon oxide component. This evidence must be also be evaluated in the light of the observation that T_g is affected and elevated by silicon oxide phase incorporation. In particular, it might be thought that the long-range chain segmental motions that are activated at T_g are implicated in degradation.

In Figure 3, it is seen that there is another DSC transition at ~ 325°C between the first and second degradative steps, the temperature of which is rather invariant with respect to the percentage of TEOS. This transition cannot be involved in major degradation, nor is it associated with crystallinity as PES is amorphous.[18]

Table II T_g and Degradation Temperatures (T_d) of PES and PES-Based Composites

Sample (%)	T_g (°C)	Step 1 T_d (°C)	Step 2 T_d (°C)	Step 3 T_d (°C)
Pure PES	210	252	433	551
90	218	232	450	552
74	213	243	440	549
50	223	250	444	546
35	226	243	439	549

Scheme II: (1) Initial Reaction of TMOS with PES Chain Ends and (2) Subsequent Silicon Oxide Phase Growth

Composite Formulation

Concept. The experiments described in this section are designed to increase the probability of having TMOS molecules undergo alcohol condensation reactions with PES chain ends before competing sol–gel reactions of TMOS molecules take place amongst themselves. The fact that the chains ends exist in dilute quantity adds to this concern. TMOS was selected over TEOS in this

case because of the greater reactivity of the former. In concept, having created PES–O–Si$(OCH_3)_3$ endgroups, and given the presence of surplus TMOS molecules, water is then added to produce silanol groups that will react with each other so that the ensuing condensation reactions result in a silicon oxide phase covalently attached to the polymer. Other than using TMOS rather than TEOS, Scheme I differs from Scheme II in that water is present at the onset in the former, whereas it is added afterward in the latter.

Formulation. Two grams of PES was completely dissolved in 10.0 mL of DMAc. 0.21 mL of TMOS (Aldrich Co., used as received), which produces the ratio of TMOS : PES equal to 9 : 1 (mol : mol), was then added to the polymer solution. 2.31 mL of 0.121*N* HCl was added to catalyze the reaction between PES–OH groups and TMOS molecules. The alcohol condensation reaction continued by refluxing the solution at 40°C for either 5 min or 3 h. Then, 0.1 mL of distilled water was added, and the solution continued to be refluxed until the total reaction time reached 6 h. The latter step

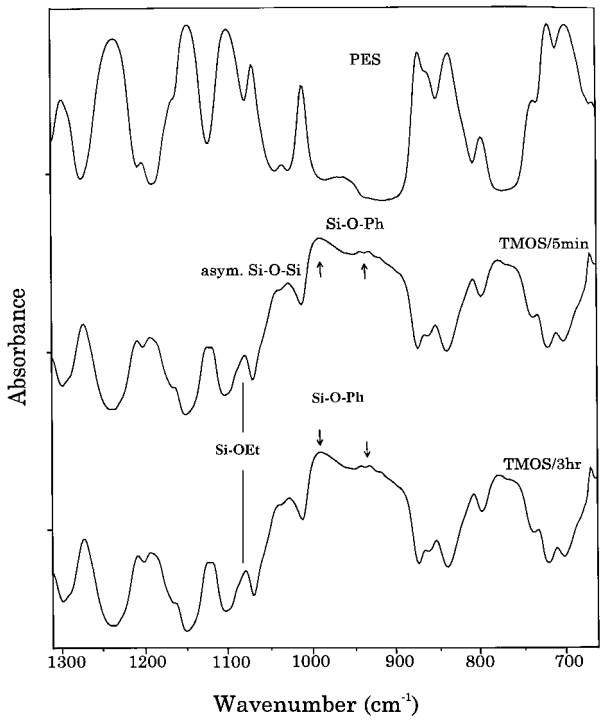

Figure 5 FTIR–ATR subtraction spectra for PES reacted with TMOS for two different times for delayed water addition, according to Scheme II. Fingerprint bands of the silicon oxide component are labeled. Also shown is the spectrum of pure PES.

Table III T_g and Degradation Temperatures (T_d) of Pure PES and PES-Based Composites

Sample	T_g (°C)	Step 1 T_d (°C)	Step 2 T_d (°C)	Step 3 T_d (°C)
Pure PES	210	252	433	551
TMOS, 5 min	221	244	446	564
TMOS, 3 h	221	258	446	562

was performed to promote condensation reactions between the partially reacted alkoxides, whereas the former steps were intended to promote endgroup reactions. The film casting process and structure–property characterizations were the same as for Scheme I.

Characterization

FTIR Spectroscopy. As seen in Figure 5, the subtraction spectra for TMOS-reacted PES showed a higher overall absorbance for the Si–O–Ph envelope than that for the Si–O–Si envelope for these samples in which alcohol condensation reactions proceeded at the chain ends for 5 min and 3 h before adding water. This order is the reverse of that for the composites formulated according to Scheme I, as seen in Figure 2. Thus, while reactions did occur between TMOS molecules producing Si–O–Si bridges, this delayed water addition procedure enhanced reactions between PES–OH groups and TMOS molecules, as desired. As in Scheme I, the signature of Si–OEt groups at 1090 cm^{-1} is present.

Differential Scanning Calorimetry and Thermogravimetric Analysis. T_g, as well as the three degradation step temperatures of these composites are listed in Table III. In the interest of brevity, the curves from which these temperatures are derived, being quite similar to those in Figures 3 and 4, respectively, are omitted. T_g is 221°C, regardless of the time of endgroup reaction before water was added. The fact that the IR spectra for these two composites in Figure 5 are practically identical suggests that allowing the preliminary reaction to proceed for 3 h is not necessary, as the same molecular structure, from the IR perspective, is attained within 5 min. While this T_g is 11°C higher than that of unfilled PES, it is only slightly higher than that for the composite prepared from the same composition (90%) using Scheme I (that is, 218°C).

TGA thermograms show that the samples for

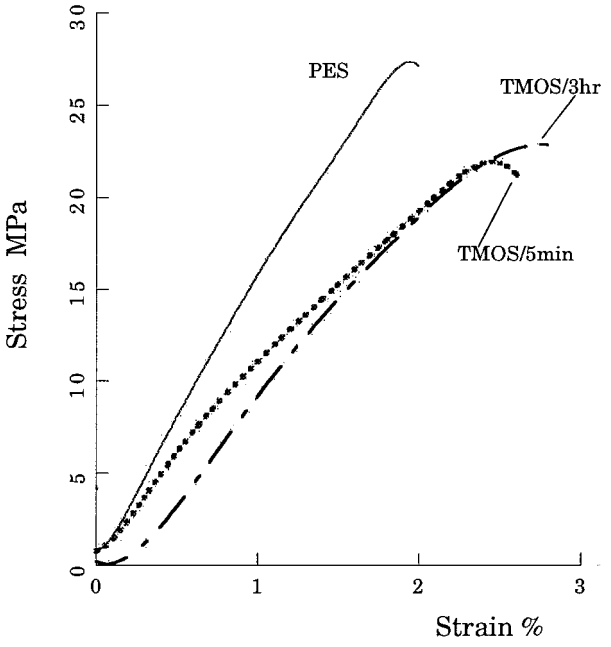

Figure 6 Tensile stress versus strain curves for PES and PES modified with TMOS according to Scheme II.

which the reaction proceeded for 3 min and 5 h prior to water addition have increased degradation temperatures relative to pure PES. Relative to the 90% composite of Scheme I, the temperature of the first degradation step increased by 12°C for 5 min, and by 26°C, for 3 h, although only the temperature of the latter is greater than that of pure PES. Second step temperatures were higher than that of pure PES, although 4°C lower than that for the 90% Scheme I composite. The temperatures of the third and most profound degradation step of the 5 min and 3 h reacted samples were significantly greater than those of the 90% Scheme I composite, as well as that of pure PES.

Mechanical Tensile Analysis. Since the composites formulated according to Scheme II appeared superior with regard to T_g, as well as thermal degradative temperature elevation, mechanical tensile analyses were performed on these samples. As seen in Figure 6, stress versus strain curves for both prewater addition times showed increased elongation-to-break, although lowered strength, as compared to unfilled PES. The curves for the two composites are similar. The increase in elongation-to-break might be rationalized in terms of an effective increase in molecular weight owing to Ph–O–Si–O–Ph linkages. Perhaps the decrease in strength is due to a disruption of the natural amorphous packing of PES chains caused by the invasive silicon oxide phase.

Scheme III: (1) Initial Reaction of TEOS with PES Chain Ends, Ethanol Addition, and (2) Subsequent Silicon Oxide Phase Growth

Composite Formulation

Concept. In the experiments described here, EtOH, a good solvent for water, was added to PES–TEOS–DMAc solutions to create a somewhat different sol–gel reaction medium from that described above. The reactions were performed (1) with EtOH addition for 3 h and (2) without EtOH for 5 min and with no water. Finally, in both cases, water is added to hydrolyze uncondensed SiOH groups to affect the growth of a silicon oxide phase that initiates, in concept, from the chain ends. The specific details of these two procedures are described below.

Formulation. 2.0 g of PES was dissolved in 10.0 mL of DMAc. 3.0 mL of EtOH (30% v/v) was added in one case, and in another case not added, to this polymer solution. 0.31 mL of TEOS (TEOS : PES equal to 9 : 1 mol : mol) was then added. 2.31 mL of 0.121*N* HCl was then added as a catalyst to both solutions. The EtOH-containing solution was refluxed at 40°C for 3 h before adding 0.1 mL of H_2O. However, for the non-EtOH-containing solution, water, in the same amount as before, was added 5 min after the addition of HCl. Then, the solutions were refluxed for 6 h total reaction time in both cases. The film casting process was the same as for the earlier experiments.

Characterization

FTIR Spectroscopy. Figure 7 consists of subtraction spectra of (a) PES reacted with TEOS for 5 min before water addition and with no added EtOH; and (b) PES reacted with TEOS for 3 h, but with added EtOH, before water addition. The two spectra are very similar, indicating similar molecular bonding throughout the silicon oxide component. As is the case for the spectra for the TMOS-reacted polymers, the Si–O–Ph envelope in Figure 7 exhibits greater absorbance relative to the Si–O–Si envelope. This signifies a considerable number of endgroup reactions. Of course, it is not possible on the basis of spectra of this quality to determine exactly what fraction of endgroup attachments form actual crosslinks. In addition to forming crosslinks, reactive —Ph–O–Si$(OEt)_3$

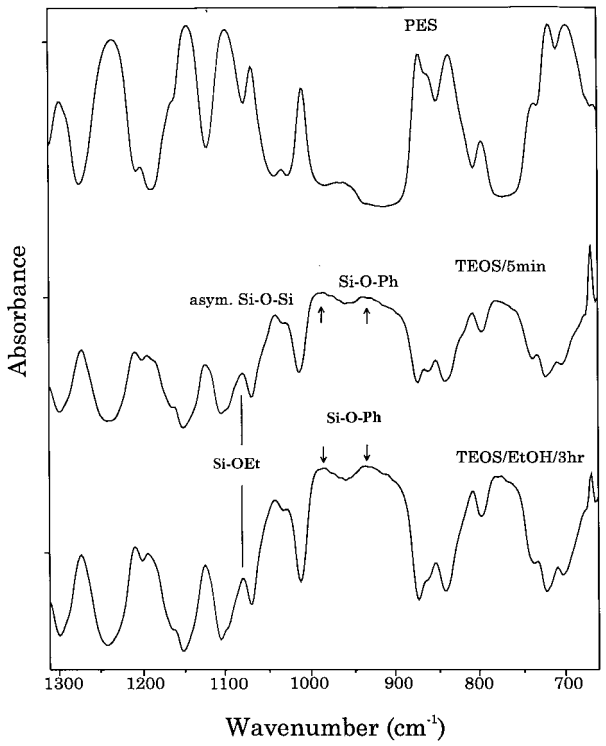

Figure 7 FTIR–ATR subtraction spectra for PES reacted with TEOS for 5 min before water addition with no EtOH, and for PES reacted with TEOS for 3 h with EtOH before water addition (Scheme III). Silicon oxide fingerprint bands are labeled. Also shown is the spectrum of pure PES.

ends can simply serve as sites from which silicon oxide nanoparticles can grow via additional condensation reactions. The composites prepared according to schemes II and III appear to contain relatively more Si–O–Ph linkages than those generated via Scheme I. Moreover, based on the relative absorbances of the two components for asymmetric Si–O–Si stretching, the silicon oxide structures seem to be more cyclic than linear in a general sense.

^{29}Si Solid-State Nuclear Magnetic Resonance Spectroscopy. The spectra for these two composites are shown in Figure 8. Noise : signal for these samples is high, which is a result of the low concentration of Si in these samples. Nonetheless, distinct resonances are seen in the Q region, particularly Q^4 and Q^3. The absence of Q^2 species is in harmony with the IR evidence, discussed above, which suggests that the incorporated silicon oxide structures are more cyclic than linear. However, in this comparison of results for the two methods, it should be realized that an IR beam in ATR mode only samples a subsurface depth of $\sim$ 1 μm, whereas the film thickness is somewhat less then 1000 μm.

Differential Scanning Calorimetry and Thermogravimetric Analysis. T_g and the temperature of each of the three steps in the degradation of TEOS-reacted PES are in Table IV. Also listed are the data for pure PES. T_g for the composite formulated using EtOH was 14°C higher than that of pure PES but is essentially the same as that for the other composite discussed in this section. However, the highest T_g of all samples inspected was that for the 35% composite listed in Table II (226°C). The highest third step degradation temperature in Table IV (562°C, for the composite formulated using EtOH) is significantly greater than that of unfilled PES but a bit lower than the TMOS-5 min composite produced according to Scheme II (564°C).

Mechanical Tensile Analysis. The composite produced using EtOH addition showed greater elongation-to-break but lower strength than pure PES; the TEOS/5 min–no EtOH composite curve is superimposed on the former curve until the stress approaches an asymptotic value before failure. We offer the same interpretations for this behavior as those given for the composites discussed above.

CONCLUSIONS

PES–[silicon oxide] hybrid materials were derived via sol–gel reactions for TEOS and TMOS in DMAc solutions of the polymer. In Scheme I, water was present at the onset so that condensation reactions amongst SiOR groups competed with SiOR reactions with —OH groups at PES chain ends. IR spectroscopy indicated formation of Si–O–Si bridges in a silicon oxide phase and PES endgroup modifications of the type Si–O–Ph. T_g was raised by as much as 16°C via restrictions on long-range chain motions by Ph–O–Si–O–Ph bridges. On the other hand, the major thermal degradation temperature was not significantly altered.

In Scheme II, the probability that TMOS molecules undergo alcohol condensation reactions with PES chain ends before competing sol–gel reactions between TMOS molecules take place was increased by adding water at a later time. IR spectra showed higher absorbance for the Si–O–Ph

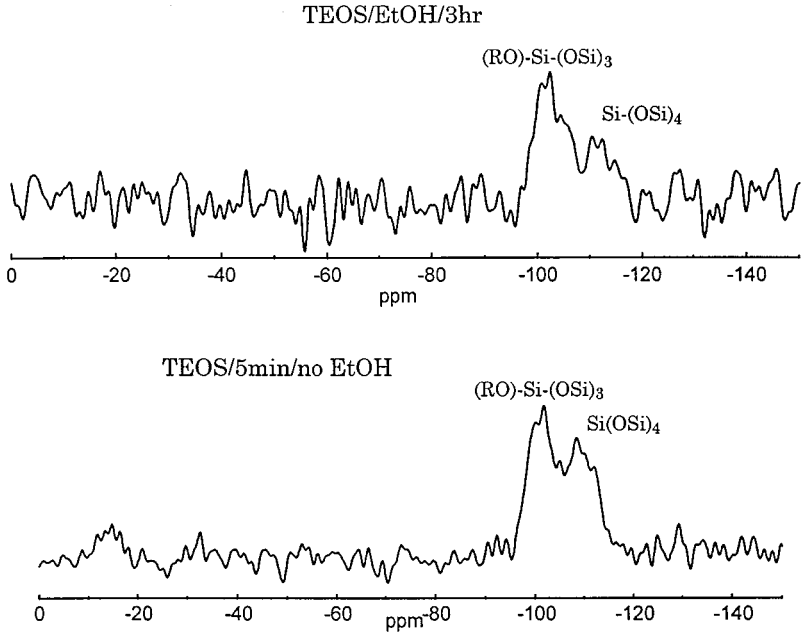

Figure 8 ^{29}Si solid-state NMR spectra for PES modified with TEOS according to Scheme III. Q^3 and Q^4 resonances are indicated.

than for the Si–O–Si group envelope. This order is the reverse of that for Scheme I composites. T_g resulting from Scheme II is 11°C higher than that of unfilled PES, and the primary degradation temperature elevated by 13°C.

Scheme III consisted of two procedures: (1) EtOH was added to PES–TEOS reactive, nonwater-containing solutions for a given time; (2) non-EtOH-containing PES–TEOS reactive solutions were also deprived of water, but for a much shorter time than in procedure (1). In a final step for both cases, water was added to hydrolyze uncondensed SiOH groups to initiate a silicon oxide phase at the chain ends. The IR spectra of these two hybrids suggest similar silicon oxide molecular bonding and considerable endgroup reactions. The composites prepared according to schemes II and III contain more Si–O–Ph linkages than those generated via Scheme I. T_g for the procedure (1) (with EtOH) composite was 14°C higher than that of pure PES; however, this value was essentially the same as that for the procedure (2) composite. The highest T_g of all samples in this study was that for the 35% composite formulated according to Scheme I (226°C).

For both scheme II and III composites, mechanical tensile tests showed increased elongation-to-break accompanied by lowered strength as compared to unfilled PES. The increased elongation-to-break is rationalized in terms of an effective increase in molecular weight owing to Ph–O–Si–O–Ph linkages.

While these exploratory experiments are incomplete, they served the primary purpose of demonstrating that the nature of PES can be inorganically modified in this fashion. A broad matrix of chemical combinations and conditions are needed to identify materials that are optimal with regard to end use properties. Electron microscopic and small angle X-ray scattering characteriza-

Table IV T_g and Degradation Temperatures (T_d) of Pure PES and PES-Based Composites

Sample	T_g (°C)	Step 1 T_d (°C)	Step 2 T_d (°C)	Step 3 T_d (°C)
Pure PES	210	252	433	551
TEOS; 5 min; no EtOH	223	248	443	557
TEOS; 3 h; in EtOH	224	247	445	562

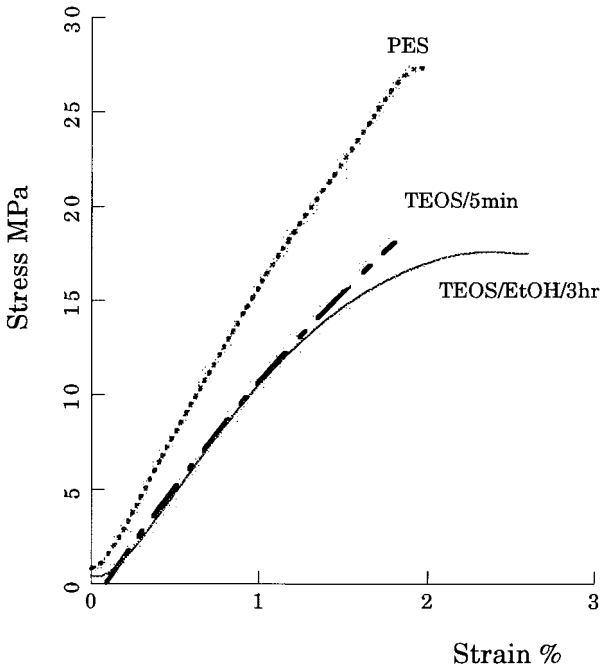

Figure 9 Tensile stress versus strain curves for PES and PES modified with TEOS according to Scheme III.

tions are needed to probe the geometry and long-range dispersion of these inorganic phases in the PES matrix.

The authors acknowledge the support of the Mississippi NSF EPSCoR program, as well as the Petroleum Research Fund (Type AC). The donation of poly(ether sulfone) materials by ICI PLC is greatly appreciated. Also appreciated is the assistance of Dr. William Jarrett, Department of Polymer Science, University of Southern Mississippi, in obtaining the ^{29}Si solid-state NMR spectra presented in this work.

REFERENCES

1. K. A. Mauritz and R. Ju, *Chem. Mater.,* **6,** 2269 (1994).
2. K. A. Mauritz and R. M. Warren, *Macromolecules,* **22,** 1730 (1989).
3. Q. Deng, R. B. Moore, and K. A. Mauritz, *Chem. Mater.,* **7,** 2259 (1995).
4. R. V. Gummaraju, R. B. Moore, and K. A. Mauritz, *J. Polym. Sci., B: Polym. Phys.,* **34,** 2383 (1996).
5. P. L. Shao, K. A. Mauritz, and R. B. Moore, *Chem. Mater.,* **7,** 192 (1995).
6. P. L. Shao, K. A. Mauritz, and R. B. Moore, *J. Polym. Sci., B: Polym. Phys.,* **34,** 873 (1996).
7. W. Apichatachutapan, R. B. Moore, and K. A. Mauritz, *J. Appl. Polym. Sci.,* **62,** 417 (1996).
8. J. Schaefer, E. O. Stejskal, and R. Buchdahl, *Macromolecules,* **10,** 384 (1977).
9. R. M. Silverstein, G. C. Bassler, and T. C. Morrill, in *Spectrometric Identification of Organic Compounds,* 4th ed.; John Wiley & Sons, New York, 1981.
10. J. E. Curry and J. D. Byrd, *J. Appl. Polym. Sci.,* **9,** 295 (1965).
11. *Spectrum of Phenoxytrimethylsilane,* Aldrich Co., Milwaukee, WI.
12. D. R. Anderson, in *Analysis of Silicones,* A. L. Smith, Ed.; Robert E. Krieger Publ. Co., Malabar, 1983, p. 254.
13. A. L. Smith, *Spectrochim. Acta* **16,** 87 (1960).
14. R. T. Conley, *Infrared Spectroscopy,* 2nd ed., Allyn and Bacon, Boston, 1975.
15. B. C. Johnson, C. Tran, I. Yilgor, M. Igbol, J. P. Wightman, D. R. Lloyd, and J. E. McGrath, *Am. Chem. Soc. Polym. Prepr.,* **24,** 31 (1983).
16. T. K. Attwood, V. J. Leslie, and J. B. Rose, *Polymer,* **18,** 369 (1977).
17. B. Crossland, G. J. Knight, and W. W. Wright, *Brit. Polym. J.,* **18,** 156 (1986).
18. J. B. Rose, *Polymer,* **15,** 456 (1974).